DESIGN, ANALYSIS AND 3D PRINTING OF A MORPHING WING PROTOTYPE

Lucian-Nicolae BAJZAT
"Transilvania" University of Braşov, Romania (lucian-nicolae.bajzat@student.unitbv.ro)

Sebastian-Marian ZAHARIA
"Transilvania" University of Braşov, Romania (zaharia_sebastian@unitbv.ro)
ORCID: 0000-0002-8636-5558

DOI: 10.19062/1842-9238.2023.21.1.1

Abstract: *In this study, two different wing morphing models were chosen for design and testing. The selected models allow for significant considerations due to their airfoil geometry variation and wingspan variation. The purpose of choosing these prototypes was to highlight the benefits of the morphing wing concept as applied to aircraft, and further applied to UAVs, as well as to light and ultra-light aircraft. In order to confirm these advantages that support the reasons for applying the concept, both structural and aerodynamic analyses were carried out. Finally, the morphing wing model with chord extension was physically manufactured by means of a 3D printing process and tested to validate the proposed concept.*

Keywords: *wing morphing, CFD analysis, finite elements analysis, 3D printing*

1. INTRODUCTION

Morphing can be defined as the ability to transform or change the shape or nature of an aircraft structure. When applied to an aircraft, this concept refers to the ability to change the shape of the wing during flight while providing an important aerodynamic advantage [1].

This change in shape occurs according to the flight mission of the aircraft or according to its flight conditions. In this way the morphing wing is defined as a wing with the capability of continuous shape change in the longitudinal plane (along the spars) or in the transverse plane (along the chord), being able to achieve this shape change in a drastic manner [2,3].

While active morphing defines the change of flight configuration through the actions of the autopilot or ground station, passive morphing refers to cases where the aerodynamic configuration is modified without the action of the autopilot or other operator [4,5].

Nowadays, 3D printing equipment is increasingly used in many fields, including engineering. Given the market and industry need, the advantages that this manufacturing process offers (reduced manufacturing time, varied additive materials, cost reduction, design optimization by using various types of fill density configurations) are the best argument for using this technology in aviation [6,7].

As expected, this technology has also been used in the aerospace industry being typically used to manufacture prototypes for parts that do not have a crucial structural role or even for ground-operated aircraft such as drones [8] and unmanned aircraft [9].

Because of the advantages of this technology, 3D printing has also been used for morphing designs. Through 3D printing of the CAD model, both 2D morphing concepts with profile modification and, more specifically, 3D concepts can be created [10,11].

2. MORPHING WING DESIGN

In order to design a morphing wing, it is necessary to take into account and consider two very important aspects: shape modification characteristics - a morphing structure must allow a well-defined shape modification, in relation to the limits of the forces acting on the model in question; structural integrity - the structure of a morphing wing differs from a conventional wing precisely by its properties of elastic shape modification. However, the designer must ensure the integrity of the assembly because it must withstand the applied stresses without buckling, fatigue or flutter. Often these two requirements are in conflict and a compromise solution must be found [12].

In order to find and implement the best option, it has been concluded that the best materials to be used in the manufacture of morphing wings are composite materials [13,14]. Composite materials have very good properties in terms of fibre orientation variation, the stiffness distribution can be adapted to cope with bending stresses. Composite materials also meet the divergence requirements in both the wingspan and chord extension directions [13,14].

Considering these aspects, two different morphing models were chosen for analysis in this paper. The first model is based on the modification of the wing geometry in terms of the aerodynamic mean chord giving a higher airfoil efficiency (Fig. 1a), and the second model shows a longitudinal extension by increasing the wingspan (Fig. 1b).

These two models use a technology that helps to achieve extension through a mechanical and an electrical system. Furthermore, the materials used are also of prime importance, as they must develop excellent elastic, thermal, physical, and mechanical properties, as they play an essential role in the designed assembly.

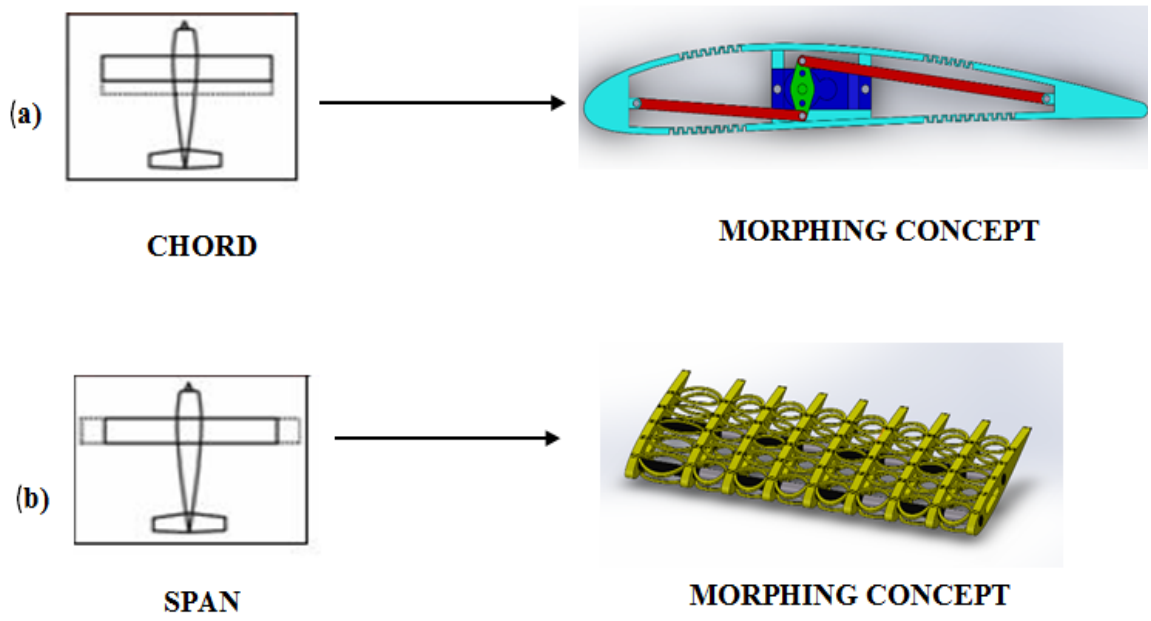

FIG. 1 Designed morphing wing models: (a) morphing model with chord extension, (b) morphing model with span extension

Morphing wing with variable (chord) profile (Fig. 2) - depending on the type and direction of deformation, this model falls into those whose aerodynamic mean chord is modified. The consequence of this modification is the increase or decrease of the aerodynamic mean chord of the model and at the same time the deformation of the airfoil from its initial position to one that gives the wing a concave or convex appearance.

In this way, by changing the airfoil shape, the wing can generate more lift when needed (usually in take-off and landing or at low speeds). For the design of this model, the NACA 4412 airfoil was initially chosen because of its good lift coefficient ratio.

The model has a length of 150 mm and a thickness of 2 mm, and the chord of this section measures 180 mm (Fig. 2a). These dimensions have been chosen in order to simplify the 3D printing procedure and at the same time to demonstrate the working principle and the benefits of the model in order to apply he prototype for a UAV.

The material chosen for this morphing wing prototype, of which the section was designed, is Nylon Alloy 910. It has excellent both physical and mechanical properties, providing extra safety to the structure. On the other hand, it also gives the elasticity needed to deform the model without suffering any defects because of this elastic deformation. To modify the shape of this prototype, a digital servo was used as the source of the mechanical system.

This digital servo is positioned on the specially designed support. The digital servo has 2 parts that have been designed: the body itself and the digital servo arm. The connections forming the chain drive from the digital servo to the designed model are represented by 2 arms. These are connected at one end by the last holes of the servo arm and at the other end by the model fasteners, thus forming the mechanical extension chain of the designed model (Fig. 2b).

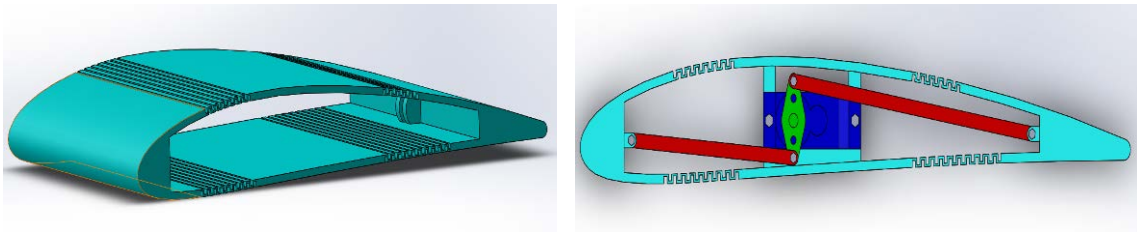

(a) (b)

FIG. 2 Variable chord morphing wing model: (a), intermediary model (b) final model

Variable span morphing wing - this model aims to lengthen the span by 12.3% from the current compressed state to the extended state (Fig. 3). Wingspan extension takes place in 4 gradual steps of equal elongation. This concept has been designed considering the stiffness of the assembly following this deformation and precisely because of this, the elongation percentage is not very high, keeping the structure rigid and safe.

The structure of this concept is made up of the following elements: 9 ribs, 4 groups of 2 ribs at symmetrical distances from each other and the ninth at a greater distance from the last group, at the tip of the wing; two cylindrical spars (main and secondary) which were also divided into 10 elements in order to place the linear actuators in those areas; the linear actuators are used to drive the longitudinal segments, making them slide and increasing the span.

There are 8 of them, positioned between the 4 pairs of ribs on both the main and secondary spars; the elastic bands maintain the shape of the ribs and stiffen the model, but also provide an additional elastic aid (20 corrugated honeycomb elastic bands); the shell is made of a thin latex film, which is a material with ideal elastic, mechanical and physical properties for this type of elastic deformation, with no risk of breakage in this case.

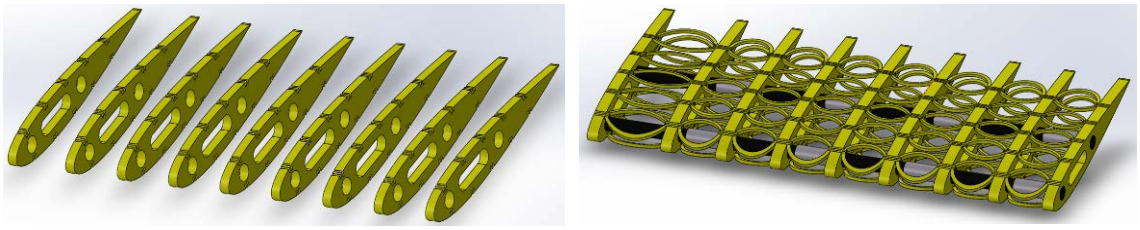

(a) (b)

FIG. 3 Variable span morphing wing model: (a) intermediary model (b) final model

In order to change the wing span, 8 piezoelectric linear actuators were used as motion sources and positioned in the area of the spar sections. The piezoelectric linear actuators are usually used in scientific and industrial applications, where high precision in motion control is required. These actuators are well known because they are often used in all modern high-tech fields including microscopy, bio-nanotechnology [15] and aerospace engineering [16,17].

3. FINITE ELEMENT ANALYSIS OF THE WING STRUCTURE

3.1 Finite element analysis of morphing wing with a variable profile

For this wing morphing concept, the finite element analysis was chosen to get results regarding the modification of the profile of the designed prototype from the initial state to the state of maximum deformation. The main goal of this morphing wing design is its future application to UAV-type aircraft or even to some ultra-light aircraft. In order to obtain relevant results in this direction, the designed prototype was scaled by a ratio of 1:6. This resulted in a wing segment with an aerodynamic profile whose chord measures 1080 mm and 900 mm in wingspan, a size close to those found on aircraft in the above-mentioned target classes. As a first step, Ansys 16.0 was chosen as the software system in which to perform these finite element analyses. The meshing of the model was carried out with an element size of 5 mm, totaling in the end 323322 elements joined by 600712 nodes. After the prototype was meshed, the fixing surfaces that will have non-deformable behavior at the analysis level and the surfaces on which the established forces are applied were determined. The fixing surface was chosen as the support of the digital servos acting on the whole wing profile modification system.

Regarding the materials used in these analyses, 3 different types of materials were selected with excellent properties in terms of flexibility and elasticity, which facilitate the deformation of the model much more easily. The materials chosen are Nylon Alloy 910, Flexifill 92A and Nylon CF 15. These materials have been added to the FEA software system by inserting some basic parameters to get the required characteristics. Since the motion generated by the digital servo gives both a concave (Fig. 4a) and a convex (Fig. 4b) deformation of the profile, both cases were analyzed.

As it can be seen, the central area is the stiffest because this is the fastened area where the digital servo is positioned. The total displacements obtained (Fig. 4c) expand in proportion to the distance from this fastening area, the maximum values being found at the model fasteners where the force is transmitted to the model. The total displacements obtained (Fig. 4d), for the convex case are about 50% smaller than in the first phase (concave case). This was predictable and natural considering that the aim of this displacement is to obtain, first of all, a part which will generate a lift force as high as possible in relation to the generated drag.

Regarding the equivalent stresses (Fig. 4e and Fig. 4f), the values are close, and for the two cases of analysis, the models withstand the applied stresses as they do not exceed the strength of the selected materials.

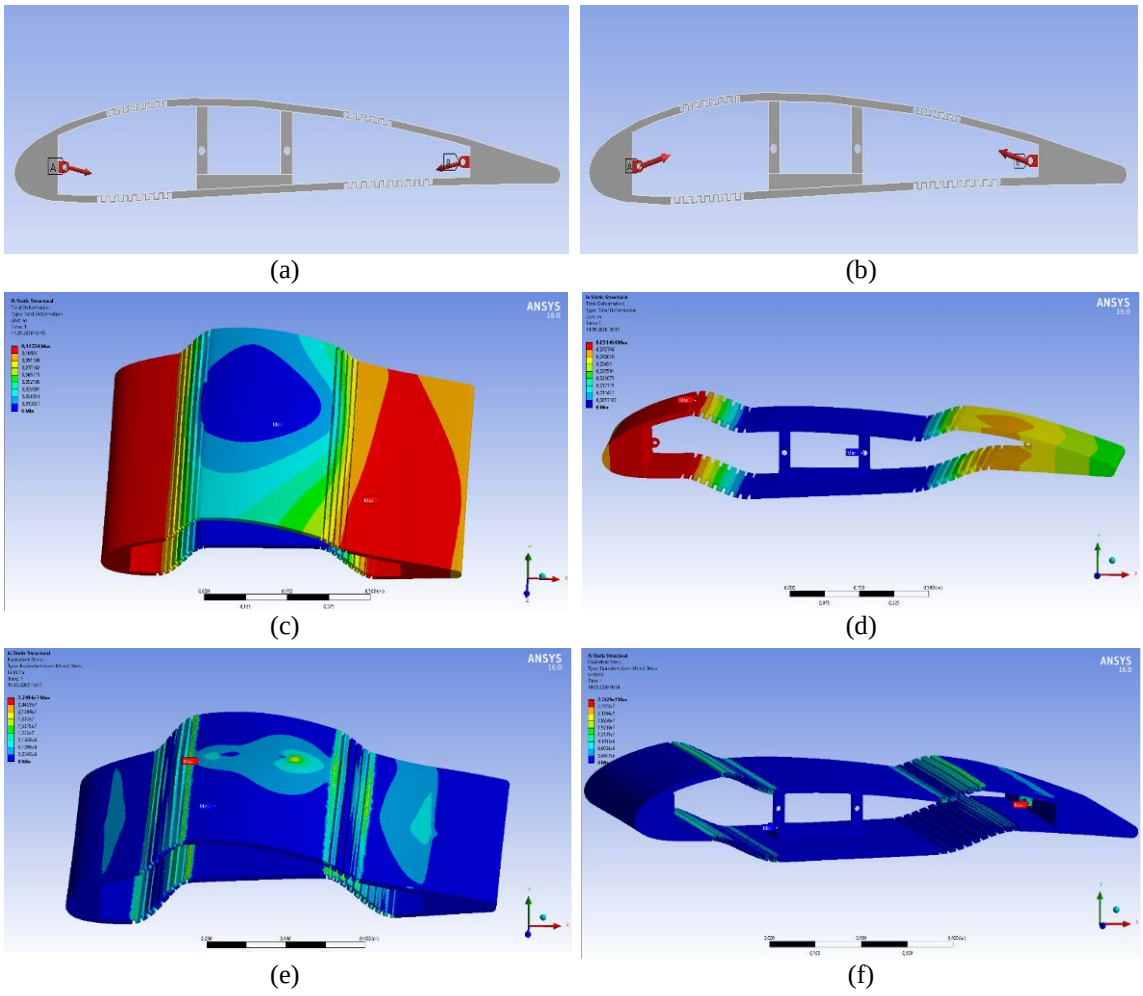

FIG. 4 Finite element analysis of the variable chord morphing wing model: (a) setting the forces for the concave shape of the model, (b) setting the forces for the convex shape of the model, (c) total displacements on the concave model, (d) total displacements on the convex model, (e) equivalent stresses on the concave model, (f) equivalent stresses on the convex model

3.2 Finite element analysis of variable chord morphing wing

For this variable span morphing wing model, a finite element analysis is performed in order to get conclusive results in terms of the displacement of elements at the structure level. Since the model is of such nature, this is the only aspect of interest for this analysis. The studied model had a dimension of 1090 mm along the airfoil chord and a span of 2565 mm.

The meshing of the model (Fig. 5a) was performed with elements of size 10 mm, resulting in a total of 154108 elements joined together by 563808 nodes. The model was fixed to the outer surface of the first rib (Fig. 5b), thus this fastening simulates the embedding of the wing in the fuselage of the aircraft.

The applied force (Fig. 5c) was calculated as the product of: the aircraft load factor (n=3.8), the gravitational acceleration (g=9.81 g/s2), the wing mass (m=92.3 kg) and the safety factor (SF=1.5), and the result is 5161.14 N.

In conclusion, the analysis of the total displacements (Fig. 5d) occurring on the structure of this variable span wing model, showed low values that do not raise problems of such nature that could lead to damage of the structure through reaching a high value of extension.

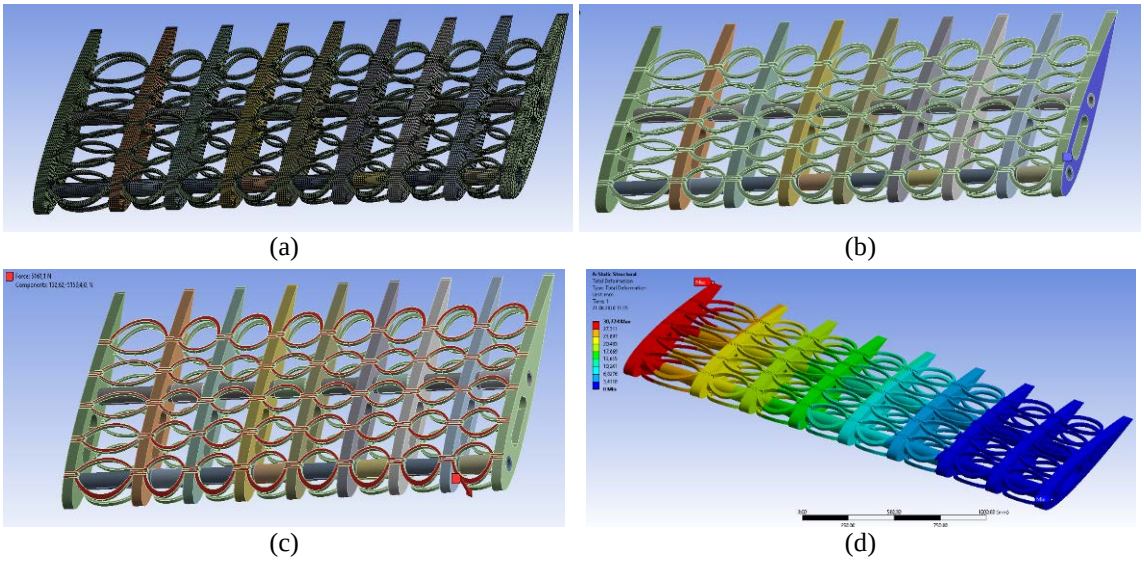

FIG. 5 Finite element analysis of the variable span morphing wing model: (a) model meshing, (b) setting boundary conditions, (c) application of stresses, (d) distribution of total displacements.

4. CFD ANALYSIS OF MORPHING WING MODELS

4.1 CFD analysis of the variable profile morphing wing

In order to carry out the aerodynamic analysis of the designed prototype using the computer-aided fluid dynamics method, the Ansys 16.0 analysis software was chosen. To carry out the CFD analysis, two reference positions where the wing profile of this concept is located were comparatively selected. The first targeted position is the neutral position of the model having as comparison the position of the model with the maximum bending shape obtained in the FEA results. Thus, the second position has a concave shape with a leading edge and trailing edge displacement of about 60 mm from the initial position.

The analysis domain, for the two models (Fig. 6a and Fig. 6b) was created in such a way that in the front of the profile there is a distance 10 times bigger than the chord of the profile, in the upper part of the profile the distance is also 10800 mm, in the lower part the same ratio of 10 times the size of the chord is kept and in the rear part of the profile the distance was set 30 times bigger than the chord. The CFD analyses were carried out for a velocity of 45 m/s, at a standard temperature of 15˚ C and an air density of 1,226 kg/m^3.

Based on the graphical representations (Fig. 6c and Fig. 6d), in both positions of the model it can be observed that the maximum pressure value is at the contact between the fluid and the prototype. If in Fig. 6c a balancing of the pressure with the atmospheric pressure is captured by the green background present in an overwhelming proportion, in Fig. 6d this area is much smaller. This indicates a higher lift force generated.

In the first phase, a rather large red area can be seen on the extrados surface indicating acceleration of the speed on the extrados surface compared to the intrados surface (Fig. 6e and Fig. 6f). At the same time, a reduced area of low velocity surface at the trailing edge can also be observed which represents the generation of low drag. In the second phase, these aspects change, and the velocity acceleration area is dramatically reduced, its

maximum value being repositioned in the leading edge area at the intrados level. On the other hand, the drag generated at the rear of the profile is much higher, an effect developed from the low speeds found at the trailing edge.

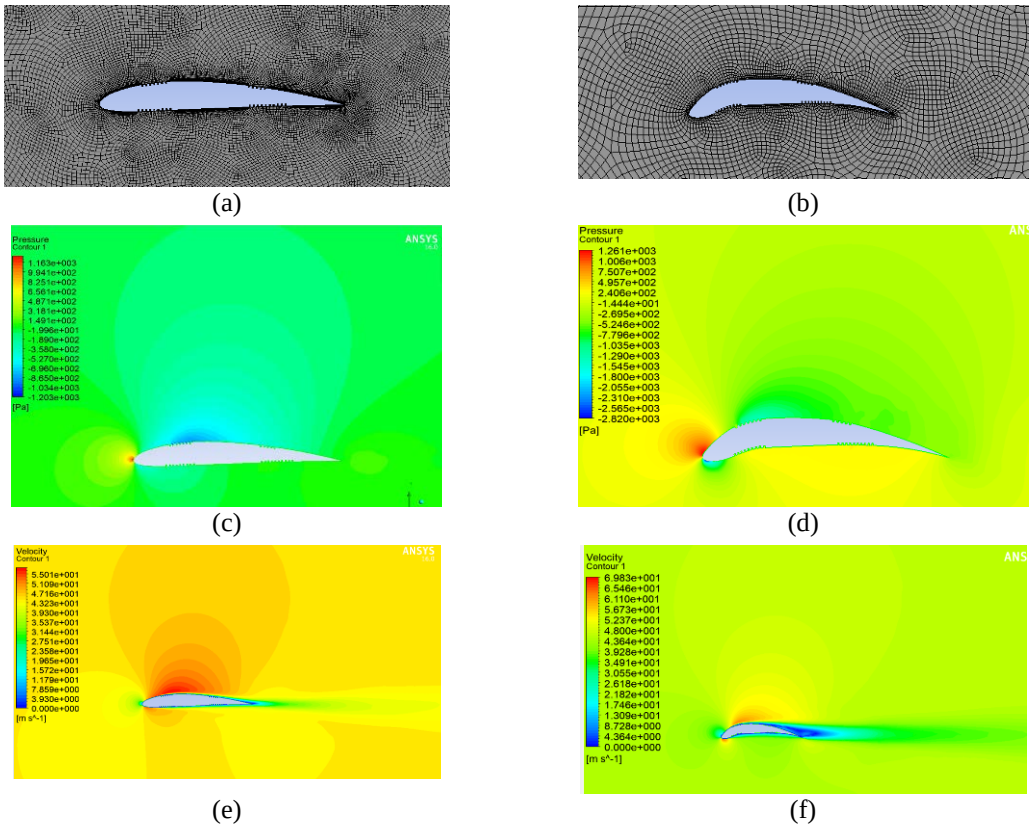

FIG. 6 CFD analysis of variable profile morphing wing: (a) meshing domain – neutral position, (b) meshing domain – deformed position, (c) pressure distribution – neutral position, (d) pressure distribution – deformed position, (e) velocity distribution – neutral position, (f) velocity distribution – deformed position

4.2 CFD analysis of the variable chord morphing wing

The aerodynamic analysis of this morphing wing prototype was carried out using the XFLR5 software system. The modelling of the wing (Fig. 7a) was done from the airfoil and using the 5 displacement positions. The purpose of these analyses (Fig. 7b) is to obtain results on the aerodynamic coefficients (lift coefficient, drag coefficient) of each of the 5 wing displacement positions (position 1 - 2565 mm; position 2 - 2655 mm; position 3 - 2745 mm; position 4 - 2835 mm; position 5 - 2925 mm). From a percentage point of view, taking into account that the wing extension from one stage to the next represents 3.51% of the initial wingspan, the percentage of total displacement amounts to a 14.04% surplus in wingspan compared to the initial position. For the wing analysis settings, a velocity of 45 m/s is entered, and the angle of attack variation was from -5˚ to 15°. This prototype variable span morphing wing offers aerodynamic advantages.

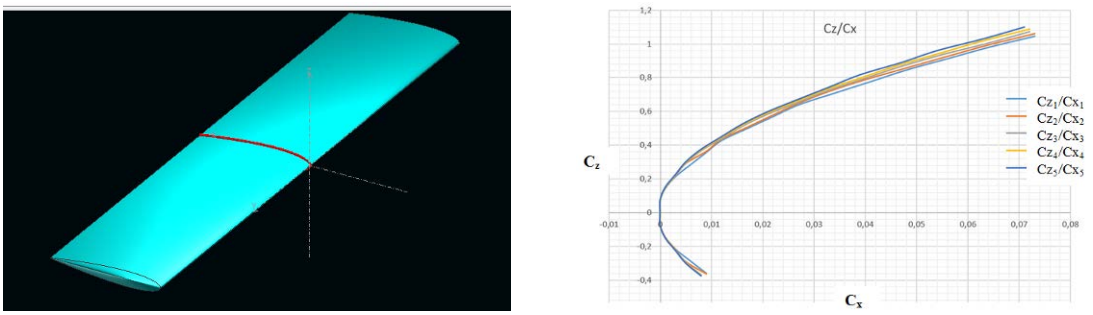

(a) (b)

FIG. 7 CFD analysis of variable chord morphing wing: (a) wing modelling, (b) variation of lift coefficient as function of drag coefficient

5. 3D PRINTING, ASSEMBLY AND OPERATION OF THE VARIABLE PROFILE MORPHING WING

Based on the FEA results, it was concluded that Flexfill 92A is the most suitable material to use to get the desired results. After the CAD model was made, it was saved and inserted into the 3D printing software system. The entire model took 40 hours and 11 minutes to complete and used 45.97 m of filament, with a part mass of 137 g (Fig. 8a). The following elements were used to manufacture the overall assembly: a nano servo controller, servo drive arm, Arduino board, adaptive nano terminal board, 4 sets of connecting wires, battery case holder, linear potentiometer, 2 connecting arms connecting the servo drive arm and the wing model, main wing structure model (Fig. 8b).

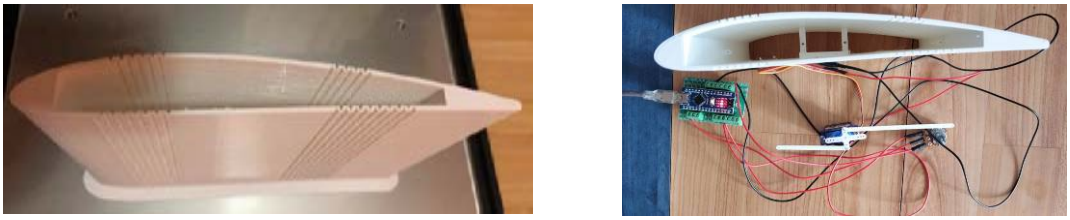

(a) (b)

FIG. 8 Manufacturing and testing of the variable chord morphing wing: (a) 3D printing of the model, (b) physical testing of the variable chord morphing wing.

From a functional point of view, this wing morphing prototype can be divided into two subdivisions. The electrical subdivision where the electrical operation of the digital servo is monitored by means of code inserted on the Arduino board and whose movements are controlled from the potentiometer, and the mechanical subdivision which aims to deform the profile because of the force transmitted from the digital servo arm to the wing itself. The electrical functional subdivision is primarily based on a code which guides the operation of this system. This code is written in Arduino software and is relatively simple. The code is inserted into the Arduino board via a cable. After testing, this system works under normal conditions. In conclusion, this system for modifying the wing to change the geometry is reliable and could be used opted in the near future.

CONCLUSIONS

Over time, due to technological development and highly flexible materials allowing for large elastic deformations, morphing concepts can bring enormous benefits both in terms of aerodynamics, controllability, economics and optimization of the flight itself. In this paper two morphing wing designs have been analyzed which focus on airfoil geometry variation and wing span variation. The structural analyses carried out on the two designs targeted different characteristics. For the airfoil morphing concept, both the equivalent stresses and the total displacements occurring in the model because of a force simulating the deformation caused by the digital servo action were investigated. For the variable span concept, the aspect of additional displacements occurring, both directionally and overall, was closely followed. From an aerodynamic point of view, for the first concept, with variable airfoil, many characteristics of the airflow on the airfoil surface both in the initial position and in a deformed position have resulted which generate a significantly higher lift force. For the second concept, according to the results obtained, it was observed that there is an aerodynamic improvement offered by this prototype. In order to validate these prototypes at the UAV aircraft level, 3D printing can be used as technological developments allow this.

REFERENCES

[1] I. Cîrciu and V. Prisacariu, Command and control of the flying wing in the morphing concept, *Review of the Air Force Academy*, no.1(23), pp. 13-18, 2013;
[2] S. C. Patel, M. Majji, B. S. Koh, J. L. Junkins, O. Rediniotisx, *Morphing wing: A demonstration of aero servo elastic distributed sensing and control*. Tec. report, Texas Institute, 2005;
[3] V. Prisacariu, I. Cîrciu and M. Boşcoianu, Morphing concept of UAVs of the swept flying wing, *Recent Journal*, vol.15, no. 1, pp. 26-33, 2014;
[4] K. Taguchi, K. Fukunishi, S. Takazawa, Y. Sunada, T. Imamura, K. Rinoie, and T. Yokozeki, Experimental study about the deformation and aerodynamic characteristics of the passive morphing airfoil, *Transactions of the Japan Society for Aeronautical and Space Sciences*, vol. 63, no. 1, pp. 18-23, 2020;
[5] C. H. U. Lingling, L. I. Qi, G. U. Feng, D. U. Xintian, H. E. Yuqing, and D. E. N. G. Yangchen, Design, modeling, and control of morphing aircraft: A review, *Chinese Journal of Aeronautics*, vol. 35, no. 5, pp. 220-246, 2022;
[6] D. W. Martinez, M. T. Espino, H. M. Cascolan, J. L. Crisostomo, and J. R. C. Dizon, A comprehensive review on the application of 3D printing in the aerospace industry, *Key engineering materials*, vol. 913, pp. 27-34, 2022;
[7] S. Singamneni, L. V. Yifan, A. Hewitt, R. Chalk, W. Thomas and D. Jordison, Additive manufacturing for the aircraft industry: a review, *Journal of Aeronautics & Aerospace Engineering*, vol. 8, no. 1, pp. 351-371, 2019;
[8] A.O. MohamedZain, H. Chua, K. Yap, P. Uthayasurian and T. Jiehan, Novel Drone Design Using an Optimization Software with 3D Model, Simulation, and Fabrication in Drone Systems Research, *Drones*, vol. 6, 2022;
[9] D. A. Popica and S. M. Zaharia, Design, aerodynamic analysis and additive manufacturing of a radio-controlled airplane, *Journal of Industrial Design and Engineering Graphics*, vol. 18, no. 1, pp. 39-44, 2023;
[10] A.E. Rivero, S. Fournier, R.M. Heeb and B.K.S. Woods, Design, Manufacture and Wind Tunnel Test of a Modular FishBAC Wing with Novel 3D Printed Skins, *Applied Sciences*, vol. 12, 2022;
[11] M. S. Parancheerivilakkathil, R. M. Ajaj and K.A. Khan, A compliant polymorphing wing for small UAVs. *Chinese Journal of Aeronautics*, vol. 33, pp. 2575–2588, 2020;
[12] T. Mkhoyan, N. R. Thakrar, R. De Breuker and J. Sodja, Morphing wing design using integrated and distributed trailing edge morphing, *Smart Materials and Structures*, vol. 31, no. 12, pp.125025 - 125045, 2022;
[13] F. Previtali, R. Bleischwitz, A. Hasse, L. F. Campanile and P. Ermanni, *Compliant morphing wing*, pp. 1–13, 22nd International Conference on Adaptive Structures and Technologies, Greece, Corfu, October 10-12, 2011;

[14] W. Johannisson, R. Harnden, D. Zenkert and G. Lindbergh, Shape-morphing carbon fiber composite using electrochemical actuation. *Proceedings of the National Academy of Sciences*, vol. 117, no. 14, pp. 7658-7664, 2020;

[15] S. M. Afonin, Structural diagram of actuator for nanobiotechnology, *Journal of Biogeneric Science and Research*, vol. 7, no. 4, pp. 1-6, 2021;

[16] M. T. Kammegne, R. M. Botez, L. T. Grigorie, M. Mamou and Y. Mébarki, A new hybrid control methodology for a morphing aircraft wing-tip actuation mechanism, *The Aeronautical Journal*, vol. 123, no. 1269, pp. 1757-1787, 2019.

[17] V. Brailovski, P. Terriault, T. Georges and D. Coutu, SMA actuators for morphing wings, *Physics Procedia*, vol. 10, pp. 197-203, 2010;